MRS Advances © 2017 Materials Research Society
DOI: 10.1557/adv.2017.367

Morphology dependent optical properties of ZnO/SiNWs nanocomposites

Aliaksandr Sharstniou[1], Stanislau Niauzorau[1], Eugene Chubenko[1], Bruno P. Azeredo[2] and. Vitaly Bondarenko[1]
[1]Belarusian State University of Informatics and Radioelectronics, 6 P. Brovki str., Minsk, Belarus.
[2]Arizona State University, The Polytechnic School, Mesa, AZ, USA.

ABSTRACT

Zinc oxide/silicon nanowires (ZnO/SiNWs) nanocomposites is a promising material for heterojunction solar cells. They combine the low-reflectivity of SiNWs, where photogenerated charge carriers are produced and harvested, and the high transparency of ZnO, which serves as a functional transparent conductive electrode. In this paper, we present a study of the anti-reflective properties of ZnO/SiNWs core-shell nanostructures. SiNWs were fabricated by a two-step metal-assisted chemical etching and coated with ZnO by electrochemical deposition. Particularly, the change in the specular reflectance of ZnO/SiNWs nanocomposites as a function of thermal annealing temperature under ambient atmosphere is investigated. First, it was shown that the reflectance in the wavelength range of 400-1000 nm of as-synthesized ZnO/SiNWs nanocomposites increases when compared to the bare SiNWs formed from Si wafers with resistivity of 0.3 and 12 Ω·cm by an 0.51 % and 0.47 %, respectively. Second, it was found that annealed ZnO/SiNWs had a 0.26 % and 0.17 % lower reflectance in the wavelength range of 400-1000 nm than as-synthesized ZnO/SiNWs and yet higher than bare SiNWs. Potential causes such results are discussed in the context of existing literature.

INTRODUCTION

Recently, research efforts have been focused on increasing the efficiency of Si-based heterojunction solar cells to provide the lowest cost per watt [1]. One of the ways to increase Si-based heterojunction solar cell efficiency is to reduce its reflection by introducing surface nanostructures such as SiNWs that effectively work as a broadband anti-reflective layer. Among all methods for nanotexturing silicon, metal-assisted chemical etching (MACE) is a simple and potentially low-cost method based solely on wet chemistry that do not involve dry-etching and lithography [2]. There are several reports on the fabrication of solar cells based on n-type SiNWs and p-type amorphous Si (a-Si) forming core-shell structures [3, 4] that highlight the longstanding effort to build improved energy harvesting devices. Though, such solar cells exhibit quite low efficiency compared to single-crystal silicon solar cells, this difference can be explained by the relative high reflectance of SiNWs/a-Si nanocomposites (approximately 15 %) [4]. Additionally, application of a-Si layers deposited by PECVD has two main disadvantages: the increase in solar cells production cost and due to a rather low electrical conductivity of the a-Si layer which has to be covered by a transparent conductive oxide, such as Al-doped ZnO, to reduce the series resistance of the solar cell. Moreover, intrinsic ZnO is a low-resistance n-type transparent semiconductor [5], which can be used simultaneously as an active layer in heterojunction solar cells [6, 7] and a conductive media for charge collection. Simulation results of such ZnO/Si heterojunction solar cells have been shown to demonstrate efficiency levels close to contemporary industrial Si solar cells [8].

Several studies of n-ZnO/p-SiNWs heterojunctions [9, 10] reported their high antireflective properties which is promising for solar cells fabrication. In order to lower production cost, ZnO deposition can be carried out via inexpensive low-temperature electrochemical methods [11, 12]. Moreover, ZnO films can be easily treated by annealing procedures to increase the crystalline quality. The annealed ZnO films demonstrate better crystallinity comparing to the unannealed films [13].

In this paper, we present the study of the antireflective properties of ZnO/SiNWs nanocomposites as a function of key material and processing parameters: wafer doping level and annealing temperature. Such nanocomposite was fabricated on a silicon wafer by forming SiNWs on its surface and, subsequently, uniformly coating it with a ZnO layer by electrochemical deposition. It has been shown that SiNWs formed by MACE exhibit low specular reflectance that does not exceed 0.04 % and 0.08 % in the wavelength range of 400-1000 nm. This result held true for SiNWs formed from Si wafers with resistivity of 0.3 and 12 Ω·cm respectively. It has been revealed that ZnO/SiNWs nanocomposites (unannealed) exhibit the specular reflectance that does not exceed 0.55 % in the wavelength range of 400-1000 nm. Subsequently, an annealing treatment was introduced to increase the crystallinity of the ZnO layer and its specular reflectance compared in the pre- and post-annealing stages. It is observed that the annealing step reduces the specular reflectance not to exceed 0.25 % and 0.3 % in the wavelength range of 400-1000 nm.

EXPERIMENT

SiNWs fabrication

SiNWs were fabricated on p-type (100)-oriented Si wafers with a resistivity of 12 and 0.3 Ω·cm using two-step MACE process. The Si wafers were immersed into an aqueous solution of 10 mM $AgNO_3$ and 2.5 M HF for 3 min. The Si samples with Ag NPs formed on their surface were etched in aqueous solution of 5 M HF and 0.3 M H_2O_2 for 1-60 min. The Ag NPs were removed from the SiNWs array using a diluted HNO_3. All procedures were performed at the room temperature (21 °C).

ZnO/SiNWs nanocomposites fabrication

ZnO was deposited into SiNWs array via the electrochemical method using two-electrode PTFE electrochemical cell. The electrochemical bath was composed of 0.03 M $ZnCl_2$ and 0.1 M KCl dissolved in dimethylsulfoxide (DMSO). The current density of 0.3 mA/cm^2 was applied for 180 min. The temperature of the solution during deposition process was 100 °C. Several samples were annealed at 750 °C for 30 min on air. Equipment used to conduct electrochemical processes was the potentiostat/galvanostat AUTOLAB PGSTAT302N. Nabertherm P330 muffle furnace was used for annealing.

ZnO/SiNWs Reflectance and Morphology Measurements

The specular reflectance spectra of ZnO/SiNWs nanocomposites were obtained using Proscan MC124 spectrophotometer with deuterium lamp as input light source under beam incidence angle of 45°. The reflectance measurements were carried out in order to study the

https://doi.org/10.1557/adv.2017.367

influence of annealing treatment on its specular reflectance by placing the detector also at an angle 45° to receive the specular component of the reflected light and, thus, not the absolute values of total reflectance. The morphology and structure of the samples were studied with the scanning electron microscope (SEM) Hitachi S-4800.

RESULTS

SiNW arrays formed by MACE on Si wafers exhibited extremely low specular reflectance over a wavelength range from 400 to 1000 nm (Fig. 1). In the MACE process, the morphology of SiNWs produced via this method strongly depends on doping level of the silicon substrate and results in dramatic changes in the reflectivity of the substrate. In figure 1, it is shown that SiNWs arrays formed from Si wafers with resistivity of 0.3 and 12 Ω·cm have a specular reflectance that does not exceed 0.04 % and 0.08 %, respectively, at wavelength range from 400 to 1000 nm. Such small relative effect of doping on reflectivity shows that the MACE process introduced minor morphological changes to the SiNWs in this doping range. This result is relevant for achieving the lowest reflectance and lowest series resistance in future efforts to build more efficient ZnO/SiNWs solar cells.

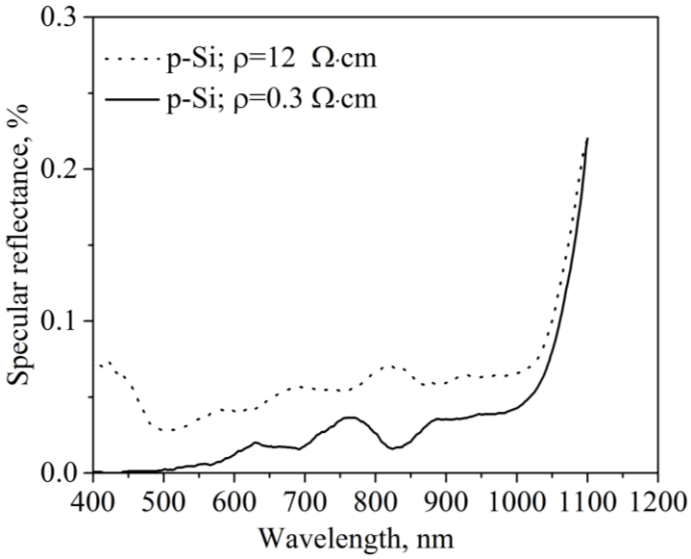

Figure 1. The specular reflectance spectra of the SiNWs formed on p-type Si wafers with resistivity 12 and 0.3 Ω·cm at a collection angle of 45°.

The uniformity and continuity of the ZnO/SiNWs composite through its thickness (of 8 μm) is of critical importance for increasing the surface area of the junction, reducing internal resistance in the composite and, thus, creating high-efficiency solar cell. In figure 2 and 3, SEM images of the cross-section of the as-synthesized ZnO/SiNWs nanocomposites (i.e. without annealing) reveal that the ZnO layer was conformally deposited over only the top half of the SiNWs array forming a core-shell structure. Meanwhile, the morphology of the composite on the lower half is comprised of discontinuous layer of ZnO nanocrystals which are located closely to each other at a pitch of approximately 5 nm (Fig. 2 and 3). Such non-uniform deposition along the SiNWs depth can be attributed to presumptive gradual depletion of the deposition solution

https://doi.org/10.1557/adv.2017.367

near the bottom of SiNWs array, which can be caused by differences in conductivities of SiNWs and deposition solution. It leads to faster electron transfer through SiNWs at its top than Zn^{2+} ions transfer at the bottom of pores. As a result the absence of Zn^{2+} ions diffused additionally to the initially present take place near the bottom of SiNWs array. In future efforts, it is critical to improve such non-uniformity through pulsed deposition methods [11].

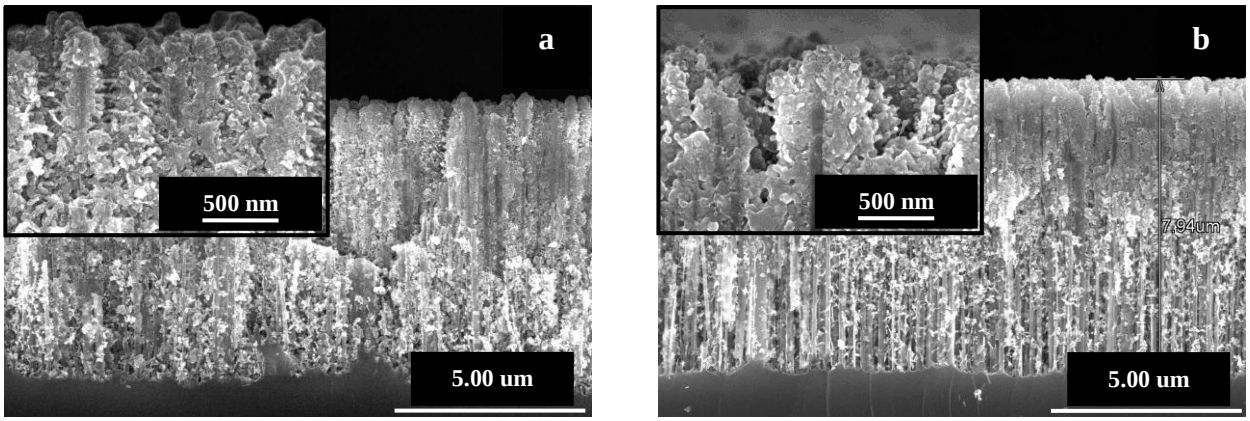

Figure 2. Cross-sectional SEM images of ZnO/SiNWs nanocomposites formed on p-type Si wafer with resistivity 0.3 Ω·cm: (a) before annealing and (b) after annealing. The insets show cross-sectional high-magnification SEM images of ZnO/SiNWs nanocomposites apexes.

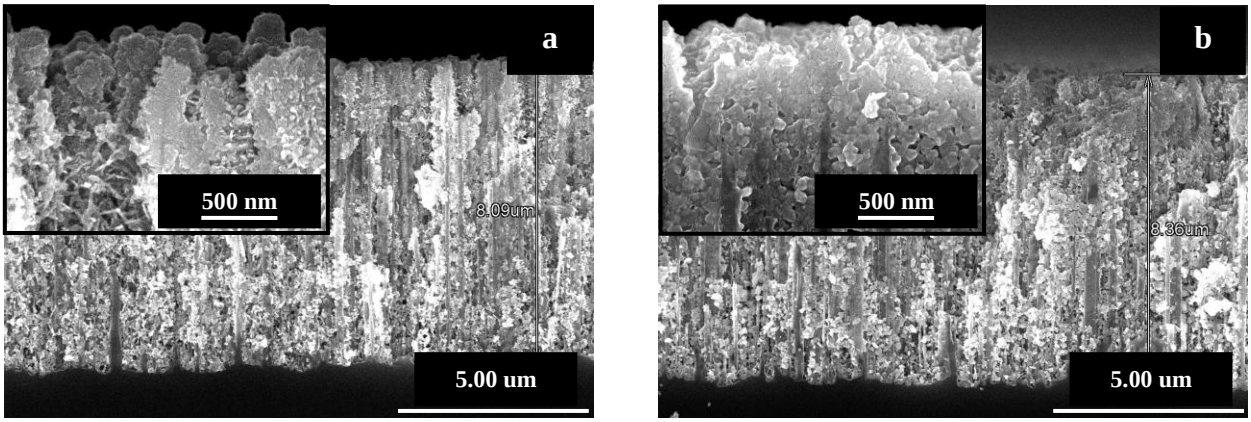

Figure 3. Cross-sectional SEM images of ZnO/SiNWs nanocomposites formed on p-type Si wafer with resistivity 12 Ω·cm: (a) before annealing and (b) after annealing. The insets show cross-sectional high-magnification SEM images of ZnO/SiNWs nanocomposites apexes.

Next, we sought to experimentally determine the effect that the annealing process alone has on the reflectivity of the ZnO/SiNWs nanocomposite. Its specular reflectance spectra was recorded before and after an annealing (Fig. 4, a and b). An increase in the reflectance of unannealed ZnO/SiNWs nanocomposite relative to that of as-synthesized SiNWs (Fig. 1) is related to the high index of refraction of the ZnO layer. Additionally, the unannealed samples demonstrated higher specular reflectance at wavelength range from 400 to 1000 nm as compared to the annealed sample. In this comparison, the reflectance is significantly reduced for wavelength range above 750 nm after annealing (Fig. 4). Such effect must be attributed to a

morphological change in the composite crystal structure and arrangement during the annealing process such as the degree of crystallinity, grain size or composition. Since high-magnification SEM images (Fig. 2 and 3 – insets) show that the average size of ZnO grains (i.e. ~ 50 nm) does not significantly change after the annealing treatment, grain size cannot explain such change in reflectance. Previous studies have shown that this exact annealing treatment increases the ZnO crystalline quality [14] which could explain this experimental observation. Another potential explanation is that metallic Zn NPs are present in the electrochemically deposited ZnO layer [15] and potentially react with oxygen impurities in the ZnO film. Although the exact mechanism for the reflectance change has not been identified, the thermal treatment improved reflectance over a relevant range of wavelengths.

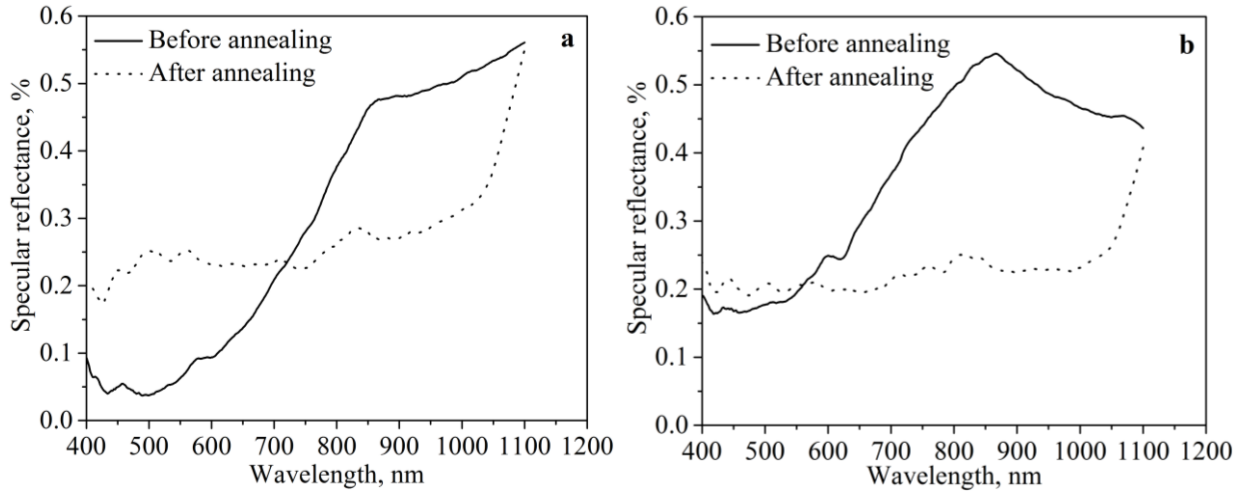

Figure 4. The specular reflectance spectra of ZnO/SiNWs nanocomposites formed on p-type Si wafer with resistivity: (a) 12 Ω·cm and (b) 0.3 Ω·cm. The collection angle is 45°.

The results on the SiNWs and ZnO/SiNWs nanocomposites reflectance properties (at wavelength range from 400 to 1000 nm) are summarized in the table I.

Table I. The specular reflectance of the SiNWs and ZnO/SiNWs nanocomposites.

Wafer resistivity (Ω·cm)	SiNWs (%)	ZnO/SiNWs (%)	Annealed ZnO/SiNWs (%)
0.3	< 0.04	< 0.55	< 0.25
12	< 0.08	< 0.55	< 0.3

CONCLUSIONS

In this work, the study of morphology-dependent optical properties of ZnO/SiNWs nanocomposites is presented. It is shown, that SiNWs arrays formed by MACE method demonstrate extremely high antireflective properties (reflectance at wavelength range from 400 to 1000 nm) which does not exceed 0.04 % and 0.08 % and weakly depends on the doping

concentration. Conformal coating of the top half-depth of SiNWs with continuous ZnO film was obtained and its specular reflectance was measured as a function of an annealing treatment. The annealing treatment of ZnO/SiNWs nanocomposites causes the decrease in the reflection. These results represent initial and concrete steps towards synthesizing ZnO/SiNWs nanocomposites with a large heterojunction area via a low-cost fabrication process. In the future work, these nanocomposites and the fabrication processes could potentially enable improvements to ZnO-Si solar cells production.

ACKNOWLEDGMENTS

This work was funded as a part of the Belarus Government Research Program "Physical materials science, novel materials and technologies", Grant 2.21.

REFERENCES

1. M. A. Green, K. Emery, Y. Hishikawa, W. Warta and E.D. Dunlop, *Prog. Photovolt.: Res. Appl.* **23**, 1-9 (2015).
2. Z. Huang, N. Geyer, P. Werner, J. de Boor, and U. Gosele, *Adv. Mater*. **23**, 285-308 (2011).
3. G. Jia, M. Steglich, I. Still and F. Falk, *Sol. Energy Mater. Sol. Cells* **96**, 226-230 (2012).
4. M. Steglich, A. Bingel, G. Jia and F. Falk, *Sol. Energy Mater. Sol. Cells* **103**, 62-68 (2012).
5. Z.L. Wang, *J. Phys.: Condens. Matter* **16**, 829-858 (2004)
6. O. Lupan, S. Shishiyanu, V. Ursaki, H. Khallaf, L. Chow, T. Shishiyanu, V. Sontea, E. Monaico and S. Railean, *Sol. Energy Mater. Sol. Cells* **93**, 1417-1422 (2009).
7. R. Pietruszka, R. Schifano, T.A. Krajewski, B.S. Witkowski, K. Kopalko, L. Wachnicki, E. Zielony, K. Gwozdz, P. Bieganski, E. Placzek-Popko and M. Godlewski, *Sol. Energy Mater. Sol. Cells* **147**, 164-170 (2016).
8. B. Hussain, A. Ebong and I. Ferguson, *Sol. Energy Mater. Sol. Cells* **139**, 95-100 (2015).
9. H. Zhou, G. Fang, L. Yuan, C. Wang, X. Yang, H. Huang, C. Zhou and X. Zhao, *Appl. Phys. Lett.* **94**, 013503 (2009)
10. W.-C. Chang, S.-C. Su and C.-C. Wu, *Materials* **9**, 534 (2016).
11. R. Jayakrishnan and G. Hodes, *Thin Solid Films* **440**, 19-25 (2003).
12. D. Gal, G. Hodes, D. Lincot and H.-W. Schock, *Thin Solid Films* **361-362**, 79-83 (2000).
13. M. Jung, J. Lee, S. Park, H. Kim and J. Chang, *J. Cryst. Growth* **283**, 384-389 (2005).
14. A. Sharstniou, E. Chubenko and V. Bondarenko, presented at *18-th International Conference-School "Advanced materials and technologies"*, Palanga, Lithuania, 2016 (unpublished).
15. Y.L. Liu, Y.C. Liu, Y.X. Liu, D.Z. Shen, Y.M. Lu, J.Y. Zhang and X.W. Fan, *Phys. B* **322**, 31-36 (2002).

https://doi.org/10.1557/adv.2017.367